ChemComm

COMMUNICATION

Check for updates

Heterostructured two-dimensional covalent organic framework membranes for enhanced ion separation†

Zhe Zhang,‡ Ankang Xiao,‡ Congcong Yin, Xingyuan Wang, Xiansong Shi [ID] * and Yong Wang [ID]

A heterostructured covalent organic framework (COF) membrane is synthesized *via in situ* linker exchange. Narrowed pores can be formed at the interface between two types of COFs by adjusting the linker exchange duration. The resultant COF membrane demonstrates a high rejection rate toward Na_2SO_4 of up to 97%.

Covalent organic frameworks (COFs) are an eminent type of framework material that feature molecularly tailorable structures and functions.[1] Two-dimensional (2D) COFs are arousing extensive attention due to their laminated structures consisting of vertically aligned channels.[2] In the past decade, 2D COFs with precisely designed pore sizes and chemistries have showcased huge promise over a wide range of fields, such as catalysis, sensing, energy storage and conversion, as well as separation.[3] Recently, considerable effort has been devoted to shaping 2D COFs into separation membranes for gas purification and water treatment.[4] In spite of this exciting progress, ion separation by 2D COF membranes poses a major challenge. Simulation studies indicate that the separation of ions by 2D COFs is viable,[5] yet it is unsatisfactory in experimental results. This divergence might arise from the disordered pores in the experimentally synthesized 2D COF membranes, as the amorphous structures still exist in some local areas inside the highly crystalline 2D COFs.[6] As a consequence, these defects would compromise the membrane selectivity to some extent.

COFs are versatile platforms in which the pore sizes and functionalities can be well tuned by means of structural control and chemistry design.[7,8] This provides an evident strategy that can be leveraged to optimize the microstructure of COF membranes, and thus substantially enhance their selectivity. For instance, the

construction of a bi-layered COF and the rearrangement of the COF orientation produced staggered stacking and vertically aligned nanopores, respectively. The effectively narrowed pores enabled a significant enhancement in sieving gas molecules.[9,10] In addition, the multiple stacking of the thin layer of the COF was reported to be effective for realizing highly efficient gas sieving.[11,12] These studies illustrate the validity of manipulating 2D COF layers to meet gas separation demands, yet the applicability in ion separation remains unexplored. Recently, we have disclosed the feasibility of bi-layered COF membranes with offset channels for desalination.[13] Thus, the pore engineering of 2D COFs paves the way for the development of high-performance membranes for ion separation.

However, the existing pore engineering of 2D COFs for enhanced separation typically relies on the successive stacking of thin layers of COF to reduce the pore size. The stacking procedure could possibly face the problem of random arrangement, thus lacking the precise control over the designated structure. This may require excessive stacking to reduce the pore size effectively, which inevitably gives rise to largely increased thickness and relatively low water permeance. Dynamic covalent chemistry describes the reversibility of chemical reactions under the conditions of equilibrium control. This intrinsic reversibility offers an opportunity that converts one form of COF into another form by linker exchange.[14] It was found that this methodology is effective in transforming amorphous polymers into crystalline COFs.[15,16] Besides, COF-to-COF transformation was also achieved from imine linkage to imide linkage by building block replacement.[17] These pioneering studies highlight an exceptional designability of COF structures through the strategy of linker exchange. With these supportive findings, we envision that the heterostructured 2D COF membranes can be synthesized by executing *in situ* linker exchange within a neat COF membrane. On the basis of dynamic covalent chemistry, the COF replacement can proceed precisely, thus allowing the controllable construction of staggered architectures with narrowed pores available for ion separation.

Herein, we report heterostructured 2D COF membranes through the partial conversion of ACOF-1 by COF-LZU1 *via*

State Key Laboratory of Materials-Oriented Chemical Engineering, College of Chemical Engineering, Nanjing Tech University, Nanjing 211816, Jiangsu, P. R. China. E-mail: xsshi@njtech.edu.cn
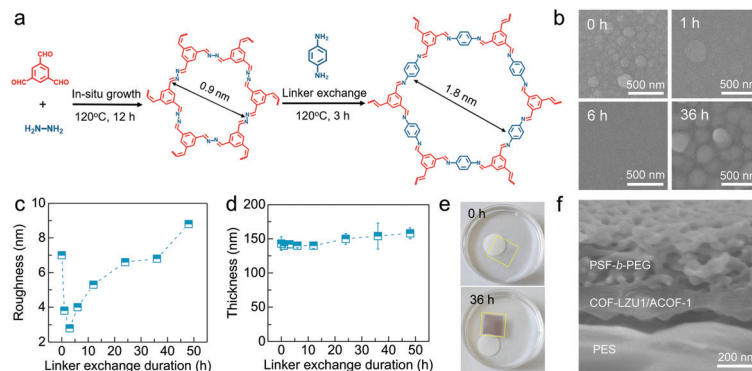
Fig. 1 Synthesis of heterostructured COF membranes. (a) Schematic diagrams of the linker exchange. (b) Surface SEM images. (c) and (d) Roughness and thickness changes *versus* linker exchange duration. (e) Photographs of the COF membranes at 0 and 36 h linker exchange. (f) Cross-sectional SEM image of the composite membrane.

in situ linker exchange (Fig. 1(a)). The neat ACOF-1 membranes were synthesized by the condensation of 1,3,5-triformylbenzene (Tb) and hydrazine hydrate (Hz) on silicon wafers under solvothermal conditions. Then, the ACOF-1 membrane was subjected to the reaction solution composed of *p*-phenylenediamine (Pa), solvents, and acetic acid to initiate the linker exchange. The surface morphology of the COF membranes was observed by scanning electron microscopy (SEM) (Fig. 1(b)). The continuous and defect-free ACOF-1 membranes can be formed at a synthesis duration of 12 h (0 h in Fig. 1(b)). The linker exchange proceeded with the adjustment of the reaction durations. By virtue of the dynamic imine linkage,[18] Hz is gradually replaced by Pa to form COF-LZU1. The morphology change of membrane surfaces confirms the occurrence of the linker exchange (Fig. 1(b) and Fig. S1, ESI†). Specifically, the SEM images show that the surface morphologies evolved from relatively rough to smooth, and then to rough again, which is consistent with the tendency of roughness variation obtained by atomic force microscopy (AFM) (Fig. 1(c) and Fig. S2, ESI†). Moreover, the inherent microstructure of COF-LZU1 may account for the larger crystal grains appearing in the membranes under prolonged linker exchange durations, which is compared to that of the neat COF-LZU1 membrane (Fig. S3, ESI†). Then, we used ellipsometry to monitor the thickness variation of the COF membranes during the linker exchange (Fig. 1(d)). Interestingly, the thickness of these membranes did not significantly change, which is in agreement with that from the SEM imaging of the cross section of the membranes (Fig. S4, ESI†). Such negligible variation in thickness may indicate that the linker exchange merely lies in the direct substitution between Pa and Hz.[15] To implement the separation, we prepared a composite membrane *via* the strategy of polymer-assisted transfer, which was proposed in our previous work.[19] The COF thin films can be easily detached from silicon wafers without cracks (Fig. 1(e) and Fig. S5, ESI†). The thin films can be tightly composited onto the macroporous poly(ether sulfone) (PES) substrate to form the composite membrane (Fig. S6, ESI†). As shown in Fig. 1(f), the resultant membrane presents a triple-layered structure, in which

polysulfone-*block*-poly(ethylene glycol) (PSF-*b*-PEG), COF-LZU1/ACOF-1, and PES serve as the protective layer, separation layer, and support, respectively. Note that the PSF-*b*-PEG layer exclusively provides the mechanical strength, and does not reject any ions because of its large mesopores.

To gain deep insights into linker exchange, we conducted a series of time-dependent characterizations. The chemical composition was studied by Fourier transform infrared spectroscopy (FTIR) (Fig. 2(a)). The characteristic peaks at 1627 cm^{-1} appeared in all the membranes, indicative of the formation of an imine linkage.[20] Moreover, the characteristic peaks at 1513 cm^{-1} assigned to phenyl groups gradually appeared as the linker exchange duration proceeded, evidencing the replacement of Hz by Pa. Given that the amount of carbon element in Pa is higher than that of Hz, we used energy dispersive X-ray spectroscopy to qualitatively analyze the variation of the amount of carbon element. As the linker exchange duration proceeded, the amount of carbon element detected in the membranes progressively increased, providing direct evidence of the occurrence of linker exchange (Fig. 2(b)). Furthermore, X-ray diffraction (XRD) was used to reveal the crystallinity variation during the linker exchange (Fig. 2(c)). In the case of the neat ACOF-1 membrane, the exclusively existing diffraction peak at ∼7.3° validates the formation of the crystalline structure.[21] As the linker exchange proceeded, the diffraction peak of ACOF-1 gradually disappeared, while the diffraction peak of COF-LZU1 at ∼4.7° appeared.[22] Moreover, at the duration of 1 and 3 h, two diffraction peaks that belong to ACOF-1 and COF-LZU1 both emerged, respectively. This indicates that a heterostructured COF membrane consisting of ACOF-1 and COF-LZU1 can be engineered by this linker exchange.[23] On the basis of the above results, we understand the engineering of heterostructured COF-LZU1/ACOF-1 membranes by linker exchange. The linker exchange starts from the membrane surface, as the bottom is sealed by the silicon wafer. Therefore, the heterostructured membrane possesses a bi-layered architecture with COF-LZU1 being fixed on the top surface of ACOF-1 (Fig. 2(d)). This unique configuration is prone to form a somewhat staggered structure, in which the
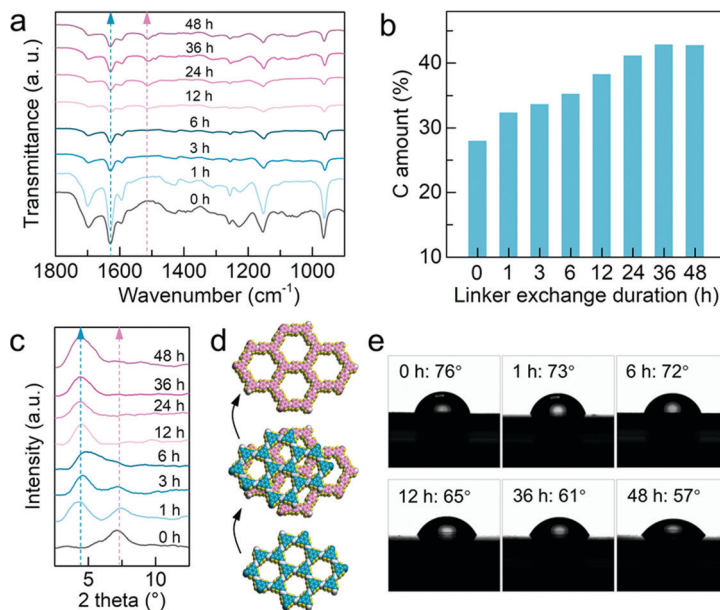
Fig. 2 Physicochemical properties of heterostructured COF membranes. (a)–(c) FTIR spectra, amounts of carbon element, and XRD patterns of heterostructured COF membranes. (d) Schematic diagrams of the structural transformation. (e) Water contact angles.

pores at the interface of COF-LZU1 and ACOF-1 can be effectively narrowed.[9] Importantly, considering that the linker exchange can be regulated by the exchange duration, the pore size of the membrane is expected to be tuned more precisely. In addition, the linker exchange also results in slightly enhanced hydrophilicity, as demonstrated by the water contact angles (Fig. 2(e)).

To acquire a narrowed pore size of the heterogeneous COF membranes, we conducted a retention test using poly(ethylene glycol) (PEG) with different molecular weights (Fig. S7, ESI†). Molecular weight cut-off is an intrinsic property of the membrane that is defined as the molecular weight at the rejection rate of 90%. The heterogeneous COF membrane exhibits a molecular weight cut-off of $\sim$510 Da (Fig. 3(a)). Furthermore, the pore size distribution can be calculated by a probability density function in terms of PEG rejection and Stokes radius.[24] It shows that the mean pore radius is centered at $\sim$0.35 nm (inset in Fig. 3(a)), which is smaller than that of ACOF-1 (pore radius = 0.45 nm), evidencing the existence of narrowed pores in the heterogeneous COF membranes. We then performed a desalination test of membranes synthesized from various linker exchange durations. Fig. 3(b) displays the water permeance and Na_2SO_4 rejection of the COF membranes with different linker exchange durations. As expected, the neat ACOF-1 membrane does not reject Na_2SO_4, which is in good agreement with previous work.[13] In contrast, after a linker exchange duration of 1 h, the membrane shows a significantly enhanced Na_2SO_4 rejection of $\sim$87%. Furthermore, the membrane exhibits high Na_2SO_4 rejection of up to $\sim$97%, after a linker exchange duration of 3 h. Prolonging the linker
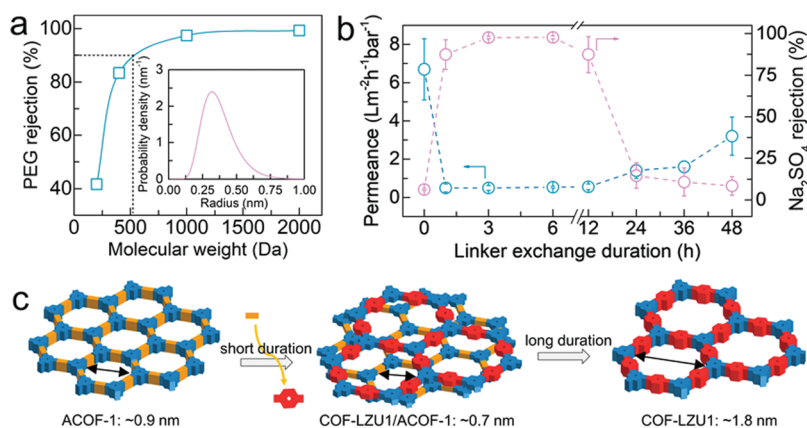

Fig. 3 Separation performance of heterostructured COF membranes. (a) PEG retention test of the membrane with a linker exchange of 3 h (inset is the pore radius distribution). (b) Water permeance and Na_2SO_4 rejection as a function of linker exchange duration. (c) Schematic diagrams of the structural transformation.

exchange duration to 6 h, the membrane still maintains its high Na_2SO_4 rejection. For water permeance, it drops with the prolonging of the linker exchange duration, because of the increased water transport resistance by the narrowed pores. Therefore, we can correlate the high Na_2SO_4 rejection and the heterogeneous structure of membranes (Fig. 3(c)). During the linker exchange process, the neat ACOF-1 was gradually replaced by COF-LZU1 *via* the exchange of Pa and Hz. In the case of partial replacement, a heterogeneous structure composed of ACOF-1 and COF-LZU1 was formed. The narrowed pores are created at the interface between them, thus rendering substantially enhanced desalination performance compared to that of the neat membrane. It is noticeable that low Na_2SO_4 rejection appeared when the linker exchange duration was prolonged from 12 to 48 h. This is mainly because of a much-pronounced replacement that transforms ACOF-1 to COF-LZU1 to a large extent, so that the relatively large pores could not reject Na_2SO_4 effectively. In addition, the relatively large pores result in gradually increased water permeance. This is in good agreement with the separation performance of the neat COF-LZU1 membrane (Fig. S8, ESI†). The separation performance of heterostructured COF membranes with a linker exchange of 3 h was tested using various inorganic salts, including $MgSO_4$, $MgCl_2$ and NaCl. The membrane exhibits high rejection rates toward Na_2SO_4 and $MgSO_4$, while relatively low rejection rates toward $MgCl_2$ and NaCl (Fig. S9a, ESI†). The membrane displays high separation factors of up to ~ 22 (Fig. S9b, ESI†), indicating a good separation selectivity toward mono/multivalent ions.

In summary, we develop a heterostructured COF membrane for ion separation. Following the mechanism of dynamic covalent chemistry, the neat ACOF-1 can be converted into COF-LZU1 *via* the exchange of the linker (Pa and Hz). It is found that partial replacement can be realized by adjusting the linker exchange duration. Therefore, a narrowed pore (pore radius, ~ 0.35 nm) is created at the interface between ACOF-1 and COF-LZU1. The resultant membrane exhibits a remarkable Na_2SO_4 rejection rate as high as 97%. Moreover, it is necessary to further optimize the microstructures of COF membranes to enhance the water permeance, which will be presented in future work. This work sheds light on the pore engineering of COFs *via* linker exchange, which may hold great potential in a wide range of applications including but not limited to separation.

Conflicts of interest

There are no conflicts to declare.

Notes and references

1 D. L. Jiang, *Chem*, 2020, **6**, 2461–2483.
2 R. Y. Liu, K. T. Tan, Y. F. Gong, Y. Z. Chen, Z. E. Li, S. L. Xie, T. He, Z. Lu, H. Yang and D. L. Jiang, *Chem. Soc. Rev.*, 2021, **50**, 120–242.
3 S. Y. Ding and W. Wang, *Chem. Soc. Rev.*, 2013, **42**, 548–568.
4 S. S. Yuan, X. Li, J. Y. Zhu, G. Zhang, P. Van Puyvelde and B. Van der Bruggen, *Chem. Soc. Rev.*, 2019, **48**, 2665–2681.
5 F. Xu, M. J. Wei and Y. Wang, *Sep. Purif. Technol.*, 2021, **257**, 117937.
6 C. J. Kang, Z. Q. Zang, A. K. Usadi, D. C. Calabro, L. S. Baugh, K. X. Yu, Y. X. Wang and D. Zhao, *J. Am. Chem. Soc.*, 2022, **144**, 3192–3199.
7 K. Y. Geng, V. Arumugam, H. J. Xu, Y. N. Gao and D. L. Jiang, *Prog. Polym. Sci.*, 2020, **108**, 101288.
8 X. S. Shi, Z. Zhang, S. Y. Fang, J. T. Wang, Y. T. Zhang and Y. Wang, *Nano Lett.*, 2021, **21**, 8355–8362.
9 H. W. Fan, A. Mundstock, A. Feldhoff, A. Knebel, J. H. Gu, H. Meng and J. Caro, *J. Am. Chem. Soc.*, 2018, **140**, 10094–10098.
10 H. W. Fan, M. H. Peng, I. Strauss, A. Mundstock, H. Meng and J. Caro, *J. Am. Chem. Soc.*, 2020, **142**, 6872–6877.
11 Y. P. Ying, S. B. Peh, H. Yang, Z. Q. Yang and D. Zhao, *Adv. Mater.*, 2021, 2104946.
12 P. Y. Wang, Y. Peng, C. Y. Zhu, R. Yao, H. L. Song, L. Kun and W. S. Yang, *Angew. Chem., Int. Ed.*, 2021, **60**, 19047–19052.
13 A. K. Xiao, X. S. Shi, Z. Zhang, C. C. Yin, S. Xiong and Y. Wang, *J. Membr. Sci.*, 2021, **624**, 119122.
14 C. Qian, Q. Y. Qi, G. F. Jiang, F. Z. Cui, Y. Tian and X. Zhao, *J. Am. Chem. Soc.*, 2017, **139**, 6736–6743.
15 D. Y. Zhu, X. Y. Li, Y. L. Li, M. Barnes, C. P. Tseng, S. Khalil, M. M. Rahman, P. M. Ajayan and R. Verduzco, *Chem. Mater.*, 2021, **33**, 413–419.
16 C. Y. Fan, H. Wu, J. Y. Guan, X. D. You, C. Yang, X. Y. Wang, L. Cao, B. B. Shi, Q. Peng, Y. Kong, Y. Z. Wu, N. A. Khan and Z. Y. Jiang, *Angew. Chem., Int. Ed.*, 2021, **60**, 18051–18058.
17 J. Maschita, T. Banerjee and B. V. Lotsch, *Chem. Mater.*, 2022, **34**, 2249–2258.
18 S. J. Rowan, S. J. Cantrill, G. R.-L. Cousins, J. K.-M. Sanders and J. F. Stoddart, *Angew. Chem., Int. Ed.*, 2002, **41**, 898–952.
19 A. K. Xiao, Z. Zhang, X. S. Shi and Y. Wang, *ACS Appl. Mater. Interfaces*, 2019, **11**, 44783–44791.
20 S. Kandambeth, B. P. Biswal, H. D. Chaudhari, K. C. Rout, H. S. Kunjattu, S. Mitra, S. Karak, A. Das, R. Mukherjee, U. K. Kharul and R. Banerjee, *Adv. Mater.*, 2017, **29**, 1603945.
21 H. W. Fan, A. Mundstock, J. H. Gu, H. Meng and J. Caro, *J. Mater. Chem. A*, 2018, **6**, 16849–16853.
22 S. Y. Ding, J. Gao, Q. Wang, Y. Zhang, W. G. Song, C. Y. Su and W. Wang, *J. Am. Chem. Soc.*, 2011, **133**, 19816–19822.
23 D. L. Ma, Q. Y. Qi, J. Lu, M. H. Xiang, C. Jia, B. Y. Lu, G. F. Jiang and X. Zhao, *Chem. Commun.*, 2020, **56**, 15418–15421.
24 S. J. Gao, Y. Z. Zhu, Y. Q. Gong, Z. Y. Wang, W. X. Fang and J. Jin, *ACS Nano*, 2019, **13**, 5278–5290.